Received 2013.12.31; Accepted
Preprint typeset using LaTeX style emulateapj v. 5/2/11

arXiv:1402.5463v1 [astro-ph.HE] 22 Feb 2014

SHORT GAMMA RAY BURST FORMATION RATE FROM BATSE DATA USING $E_P - L_P$ CORRELATION AND THE MINIMUM GRAVITATIONAL WAVE EVENT RATE OF COALESCING COMPACT BINARY

Daisuke Yonetoku[1], Takashi Nakamura[2], Keitaro Takahashi[3], and Asuka Toyanago[1],

Received 2013.12.31; Accepted

ABSTRACT

Using 72 Short Gamma Ray Bursts (SGRBs) with well determined spectral data observed by BATSE, we determine their redshift and the luminosity by applying E_p–L_p correlation for SGRBs found by Tsutsui et al. (2013). For 53 SGRBs with the observed flux brighter than 4×10^{-6} erg cm^{-2}s^{-1}, the cumulative redshift distribution up to $z = 1$ agrees well with that of 22 *Swift* SGRBs. Especially good agreement is seen for $z < 0.4$ with the KS chance probability of 5.3%. This suggests that the redshift determination by the E_p–L_p correlation for SGRBs works very well. The minimum event rate at $z = 0$ is estimated as $R^{\rm min}_{\rm on-axis} = 2 \times 10^{-10}$ events Mpc^{-3}yr^{-1} so that the minimum beaming angle is $0.57^\circ - 3.6^\circ$ assuming the merging rate of $10^{-7} - 4 \times 10^{-6}$ events yr^{-1}galaxy^{-1} suggested from the binary pulsar data. Interestingly, this angle is consistent with that for SGRB130603B of $\sim 4^\circ - 8^\circ$(Fong et al. 2013b). On the other hand, if we assume the beaming angle of $\sim 6^\circ$ suggested from four SGRBs, the minimum event rate including off-axis SGRBs is estimated as $R^{\rm min}_{\rm all} \sim 4 \times 10^{-8}$ events Mpc^{-3}yr^{-1}. If SGRBs are induced by coalescence of binary neutron stars (NSs) and/or black holes (BHs), this event rate leads to the minimum gravitational-wave detection rate of 1.3(50) events y^{-1} for NS-NS (NS-BH) binary, respectively, by KAGRA, adv-LIGO, adv-Virgo and GEO network.

Subject headings: gamma-ray burst; short gamma-ray burst; gravitational wave

1. INTRODUCTION

In 2004, Yonetoku et al. (2004) analyzed data of 16 Long Gamma-Ray Bursts (LGRBs) observed by BATSE and BeppoSAX with known redshifts, and obtained the peak energy E_p of the time integrated spectrum. They found the $E_p - L_p$ correlation between the E_p and the peak luminosity L_p integrated for 1 s time interval at the peak as

$$L_p = 2.34 \times 10^{51} \mathrm{erg\ s^{-1}} (\frac{\mathrm{E_p}}{100\mathrm{keV}})^2. \quad (1)$$

The linear correlation coefficient of the $\log E_p - \log L_p$ correlation is 0.958 and the chance probability is 5.31×10^{-9}. Ghirlanda et al. (2005a,b); Krimm et al. (2009); Yonetoku et al. (2010) checked the properties of the $E_p - L_p$ correlation and confirmed its reliability. Using this tight $E_p - L_p$ correlation, Yonetoku et al. (2004) determined the redshift and the peak luminosity for 689 bright BATSE LGRBs without known redshift and found that LGRBs with redshift greater than $z > 8$ and possibly up to $z \sim 12$ might exist. In reality in 2009, GRB 090423 at $z = 8.26$ was found (Tanvir et al. 2009). They also showed that the integrated luminosity function $\Psi(L)$ obeys the broken power-law as $\Psi(L) \propto L^{-0.29}$ for lower L and $\Psi(L) \propto L^{-1.02}$ for higher L. As for the GRB formation rate, they found that it increases up to $z \sim 1$ with increasing z and, then, does not decrease significantly up to $z \sim 10$.

As for Short Gamma Ray Bursts (SGRBs), however, due to the small number of the events with known redshifts and the good spectra to determine E_p, it has been difficult to do a similar analysis to those done for LGRBs. Recently, Tsutsui et al. (2013) succeeded in determining $E_p - L_p$ correlation for SGRBs. They used 8 secure SGRBs out of 13 candidates and obtained

$$L_p = 7.5 \times 10^{50} \mathrm{erg\ s^{-1}} (\frac{\mathrm{E_p}}{100\mathrm{keV}})^{1.59}, \quad (2)$$

where E_p is from the time integrated spectrum again while L_p was taken as the luminosity integrated for 64ms time intervals at the peak considering the shorter duration of SGRB. The linear correlation coefficient of the $E_p - L_p$ correlation is 0.98 and the chance probability is 1.5×10^{-5}. Although the $E_p - L_p$ correlation for SGRBs is not so tight as that for LGRBs due to the fact that the number of SGRBs is half of that of LGRBs, it is accurate enough to use it as a distant indicator for many SGRB events without known redshifts due to the lack of observations of afterglows. Note here that for the same $E_p = 100(1000)$ keV, SGRB is $\sim 3(8)$ times dimmer than LGRBs, respectively.

In this Letter, we determine the redshifts of SGRBs observed by BATSE using the $E_p - L_p$ correlation mentioned above. Then, we obtain the luminosity function and SGRB formation rate. This Letter is organized as follows. In §2 , we describe the observations and data analyses. After that, we show the redshifts estimated by $E_p - L_p$ correlation for SGRBs and obtain the cumulative redshift distribution and compare it with the observed one. We also show the cumulative luminosity function and the SGRB formation rate as a function of

yonetoku@astro.s.kanazawa-u.ac.jp
takashi@tap.scphys.kyoto-u.ac.jp
[1] College of Science and Engineering, School of Mathematics and Physics, Kanazawa University, Kakuma, Kanazawa, Ishikawa 920-1192, Japan
[2] Department of Physics, Kyoto University, Kyoto 606-8502, Japan
[3] Faculty of Science, Kumamoto University, Kurokami, Kumamoto, 860-8555, Japan

redshift. §3 is devoted to discussions and implications of the results.

2. OBSERVATIONS & DATA ANALYSES

2.1. *Data Selection*

We used the BATSE current burst catalog which contains 2704 GRBs during its life time ($\sim$ 9.2 years) in orbit. The average fraction of sky coverage of BATSE instruments is 0.483, so the effective life time is ~ 4.4 years for the entire sky. We selected events with the short time duration of $T_{90} < 2$ sec in the observer frame as SGRB candidates. Here T_{90} is measured as the duration of the time interval during which 90 % of the total observed counts have been detected. After that, we selected the brightest 100 SGRBs in 1,024 ms peak photon flux. The peak flux of all events we selected is brighter than 1 photons cm^{-2}s^{-1}. The trigger efficiency of BATSE instrument is almost 100 % (larger than 99.988 %), so we can estimate SGRB rate without any correction in this point.

2.2. *Spectral Analyses*

We used spectral data detected by the BATSE LAD detectors and performed the standard data reduction method. Then we succeeded in analyzing spectral data for 72 events. The other 28 events are statistically poor or the variable background condition, so we failed to obtain spectral parameters for the standard analyses.

We used the spectral model of the smoothly broken power-law model, so called Band function (Band et al. 1993) as following;

$$N(E) = \begin{cases} A\Big(\frac{E}{100\ \mathrm{keV}}\Big)^{\alpha} \exp(-\frac{E}{E_0}) \\ \text{for } E \le (\alpha-\beta)E_0, \\ A\Big(\frac{E}{100\ \mathrm{keV}}\Big)^{\beta} \Big(\frac{(\alpha-\beta)E_0}{100\ \mathrm{keV}}\Big)^{\alpha-\beta} \exp(\beta-\alpha) \\ \text{for } E \ge (\alpha-\beta)E_0, \end{cases} \quad (3)$$

where, $N(E)$ is in unit of photons cm^{-2}s^{-1}keV^{-1}. The spectral parameters of α, β and E_0 is the low- and high-energy index, and the energy at the spectral break, respectively. For the case of $\beta < -2$ and $\alpha > -2$, the peak energy can be derived as $E_p = (2+\alpha)E_0$. In previous work, although Ghirlanda (2009) performed spectral analyses for 79 SGRBs with cutoff power-law model, we used the Band function for all events in this work. If we can not determine the high energy spectral index β, we fixed the parameter as $\beta = -2.25$ which is average value of bright events. Comparing the E_p values of both Ghirlanda (2009) and this work, we confirmed both results are strongly correlate with each other while our E_p is slightly smaller than their results. This is recognized as the difference of model function as Kaneko et al. (2006) mentioned. That is, cut off power-law tends to have larger E_p than that by the Band function.

2.3. *Redshift Estimation for SGRBs*

For long GRBs, there are well known correlations between E_p and brightness like Amati – Yonetoku – Ghirlanda correlations (e.g. Amati et al. 2002; Yonetoku et al. 2004; Amati 2006; Ghirlanda et al. 2004; Yonetoku et al. 2010). Recently Tsutsui et al. (2013) reported the E_p–luminosity correlation in SGRBs as

$$L_p = 10^{52.29}\Big(\frac{E_p}{774.5\ \mathrm{keV}}\Big)^{1.59} \quad \mathrm{erg\ s^{-1}}. \quad (4)$$

This is ~ 5 times dimmer than the E_p–luminosity correlation of long GRBs. This equation can be rewritten as

$$\frac{d_L^2}{(1+z)^{1.59}} = \frac{10^{52.29}}{4\pi F_p}\Big(\frac{E_p}{774.5\ \mathrm{keV}}\Big)^{1.59} \quad \mathrm{erg\ s^{-1}}. \quad (5)$$

As Yonetoku et al. (2004) performed, using the observed E_p and 64 msec peak flux, we can estimate the pseudo redshift, and calculate the luminosity distance for each event. Then we used the cosmological parameters of $\Omega_m = 0.3$, $\Omega_\Lambda = 0.7$ and Hubble parameters of $H_0 = 71$ km s^{-1}Mpc^{-1}.

We succeeded in calculating all pseudo redshifts for 72 events. In figure 1, we show the data distribution on the plane of redshift and peak luminosity. The filled squares and circles are known redshift samples and pseudo redshift samples, respectively. The solid line is the flux limit of 4×10^{-6} erg cm^{-2}s^{-1} we used.

To confirm if our redshift determination is consistent with one of the known redshift SGRBs, we compared the cumulative redshift distributions of both samples. In figure 2, we show the cumulative redshift distribution of 22 observed SGRBs of $z \le 1.13$ (Fong et al. 2013a) and our 45 BATSE SGRBs brighter than the flux limit and with the pseudo redshift of $z \le 1.14$ in figure 1. [4] The reason we set upper bound of the redshift comes from the small number (only one) of the known redshift SGRB larger than $z = 1.13$. The black and the gray solid lines in figure 2 show 45 BATSE SGRBs in this paper and 22 known redshift SGRBs detected by HETE-2 and *swift*/BAT, respectively. The Kolmogorv-Smirnov test shows the probability of null-hypothesis is 79.4 %. Remarkably, focusing the lower redshift range of $z \le 0.4$, the Kolmogorv-Smirnov test shows the probability of 94.7 %. We can recognize these probabilities are enough high for the number of events of both datasets. Therefore we conclude these two curves show the almost same distribution, and the E_p–L_p correlation for SGRBs (Tsutsui et al. 2013) is a good distance indicator. Hereafter we use 53 SGRBs above the flux truncation of 4×10^{-6} erg cm^{-2}s^{-1} with maximum redshift $z = 2.2$ to estimate the SGRB formation rate in the next section.

2.4. *SGRB Formation Rate*

The statistical problem to estimate the true SGRB formation rate and luminosity functions is how to deal the data set truncated by the flux limit. In many cases, assuming some parametric forms (model functions) for the luminosity function and redshift distribution, all parameters are simultaneously estimated to fit the data distri-

[4] In Table 3 of Fong et al. (2013a), 37 SGRBs are listed. However 11 SGRBs have either no firm redshift information, for example, two redshift candidates or only upper/lower limits of the redshift. Moreover we removed three possible host-less SGRBs because their redshift is measured by the absorption lines in the optical afterglow and they may be smaller than the real redshift. We removed the most distant SGRB of $z = 2.609$ to keep the shape of cumulative distribution. Finally, we use only 22 SGRBs.

bution of the flux limited samples. However, if we use the model function far from the true distribution, we may obtain unrealistic solutions for each parameters. Especially, we have little knowledge about the functional form of SGRB formation rate and it may be different from the general star formation rate. Therefore it is preferable to use a non-parametric methods.

In this paper, we used a non-parametric method by Lynden-Bell (1971); Efron & Petrosian (1992); Petrosian (1993); Maloney & Petrosian (1999) developed to estimate the redshift distribution of Quasar samples. This method is also used in the long GRBs (e.g. Lloyd-Ronning, Petrosian & Mallozzi 2001; Yonetoku et al. 2004; Dainotti, Petrosian, Singal et al. 2008). The details of methodologies are found in these papers so that we briefly summarized the thread of data analyses to estimate the luminosity function and the SGRB formation rate independently.

First of all, we estimate the correlation between the redshift and the luminosity with the assumption of the functional form of luminosity evolution $g_k(z) = (1+z)^k$. Then we searched the appropriate k-value which gives the τ-statistical values (similar to Kendall τ rank correlation coefficient) to be zero. It means that the data set $(z, L/g_k(z))$ have no luminosity evolution, and z and $L/g_k(z)$ become independent parameters each other. Since we estimated $k = 3.3^{+1.7}_{-3.7}$ with 1 σ uncertainty, we assume no-luminosity evolution in this analyses.

Next, we can separately calculate the luminosity function for $L/g_k(z)$ and the SGRB formation rate as a function of redshift with non-parametric method. We have already removed the effect of luminosity evolution (in this paper we found no-evolution as $g_k(z) = 1$), a unique formula for the luminosity function can be adopted for all redshift range. Then, we can easily estimate the number of events lower than the flux limit, and also obtain the SGRB formation rate.

In figure 3, we show the cumulative luminosity function of $L/g_k(z)$. In long GRBs, several authors reported the luminosity function can be described as broken power-law (e.g. Yonetoku et al. 2004). However we can not find obvious break structure in figure 3, and it can be almost fitted by a simple power-law with the index of -0.94.

In figure 4, we show the SGRB formation rate per comoving volume and the proper time as a function of $(1+z)$. Here, we used the BATSE's effective observation period of 4.4 years as already explained in section 2.1. This SGRB rate is calculated for the events with the peak luminosity of $L > 10^{50}$ erg s^{-1} in observer's frame. The functional form can be described as

$$\rho_{\rm SGRB}(z) \propto \begin{cases} (1+z)^{9.4^{+0.8}_{-1.0}} & \text{for } (1+z) < 1.55, \\ \text{const.} & \text{for } (1+z) \geq 1.55. \end{cases} \quad (6)$$

The local minimum event rate at $z = 0$ is about $\rho_{\rm SGRB,0} = 2 \times 10^{-10}$ events Mpc^{-3}yr^{-1}. Here, in this figure, we assume that the radiation of SGRB's prompt emission is isotropic, and we do not include any geometrical correction for the jet opening angle. In this analysis, we treated SGRB samples with the observed flux larger than 4×10^{-6} erg cm^{-2}s^{-1} and dimmer SGRBs are not included. Therefore the SGRB formation rate estimated here is regarded as the minimum value.

Let us assume that progenitor of SGRBs is the merging neutron star-neutron star (NS-NS) binary here. Kalogera et al. (2004a,b) obtained the probability function of the rate of the merging NS-NS binary taking into account the observed NS-NS binary, the beam factor of the pulsar, pulsar search time, the sensitivity and so on. They obtained a merging rate of $R_{\rm m} = 10^{-7} - 4 \times 10^{-6}$ events y^{-1}galaxy^{-1} with 99% confidence level. [5]. From $\rho_{\rm SGRB}(0)$ and $R_{\rm m}$, we can determine the minimum jet opening angle $\theta_j^{\rm min}$ by

$$1 - \cos\theta_j^{\rm min} = \frac{\rho_{\rm SGRB,0}}{R_{\rm m}} \quad (7)$$

Then $\theta_j^{\rm min} = 0.57°$–$3.6°$ at the 99 % confidence level.

3. DISCUSSION

Long GRBs(LGRBs) are believed to be caused by relativistic jets since the break of the afterglow light curves are seen for many LGRBs. The typical example is GRB990510 which shows achromatic break of the afterglow light curve (Harrison et al. 1999). The physical reason for the achromatic break of the light curve comes from the jet dynamics after the Γ factor of the jet becomes smaller than the inverse of the jet opening angle (Rhoads 1999). If SGRBs are also caused by relativistic jets, we can expect a jet break similar to that of LGRBs. However, so far, only GRB130603B has multi-wavelength data from radio to X-ray to confirm the achromatic jet break of the afterglow. Fong et al. (2013b) determined the jet opening angle of GRB130603B as $4° - 8°$, where the ambiguity comes from the uncertainty in the kinetic energy of the jet and the ambient gas density. Very interestingly, the opening angle of GRB130603B is compatible with the minimum jet opening angle derived in the previous section.

For GRB 051221, the steepening of the afterglow light curve was observed in X-ray band at $t \sim 5$ days. If we identify this steepening as the jet break, the jet opening angle is determined as $5.7° - 7.3°$ (Soderberg et al 2006). For GRB111020A, Fong et al. (2012) argued a significant break at $t \sim 2$ days in X-ray band and obtained the jet opening angle of $3° - 8°$. For GRB090426, Nicuesa Guelbenzu et al. (2011) obtained the jet opening angle of $4.4°$ from a break at $t = 0.4$ day. The other jet opening angle information from SGRBs is lower limits (see section 8.4 of recent review by Berger (2013)) so that we use only these four estimations of the jet opening angles. A simple average of these four angles is $\sim 6°$. Taking this value, then, the event rate of SGRB including the off-axis ones becomes $R_{\rm all}^{\rm min} = 3.6 \times 10^{-8}$ events Mpc^{-3}yr^{-1}.

Now let us assume that the central engine of SGRB is a coalescence of a neutron star-neutron star (NS-NS) binary. Then, we can obtain an estimate of the event rate of gravitational-wave detection. The detectable range of KAGRA [6], adv-LIGO [7], adv-VIRGO [8] and GEO [9] network is ~ 200 Mpc so that the minimum gravitational-wave detection rate is obtained as ~ 1.3 events yr^{-1}.

[5] There are errors in Kalogera et al. (2004a) so that the correct one is given in Kalogera et al. (2004b)
[6] http://gwcenter.icrr.u-tokyo.ac.jp/en/
[7] http://www.ligo.caltech.edu/
[8] http://www.ego-gw.it/index.aspx/
[9] http://www.geo600.org/

This is an estimate independent of the one based on pulsar observations (Kalogera et al. 2004a,b). On the other hand, if the central engine of SGRBs is a coalescence of a black hole-neutron star (BH-NS) binary with masses, say $M_{\rm BH} = 10M_\odot$ and $M_{\rm NS} = 1.4M_\odot$, the detectable range will become ~ 3.4 times larger because it is proportional to $M_{\rm chirp}^{5/6}$, where the chirp mass $M_{\rm chirp}$ of a binary is defined by $M_{\rm chirp} = (M_1M_2)^{3/5}/(M_1+M_2)^{1/5}$ (Seto, Kawamura & Nakamura 2001) where M_1 and M_2 are the masses of each compact object. In this case, the detection rate will be ~ 50 events yr^{-1}.

In the above estimation, we used the BATSE SGRBs with a flux larger than 4×10^{-6} erg cm^{-2}s^{-1} which is shown by the solid line in Fig. 1. As is seen in Fig.1, there are 17 events below the flux limit and the event with the lowest fluxes located a factor of ~ 4 below the solid line. If we lower the flux limit by a factor of 4, noting that the cumulative luminosity function is proportional to L^{-1} as seen in Fig. 3, we can expect that the event rate can be a factor ~ 4 larger. Then the gravitational-wave detection rate becomes 5(200) events y^{-1} for NS-NS (NS-BH) binary, respectively.

Coward et al. (2012) analyzed 14 *Swift* SGRBs taking into account the ratio of the rate of BATSE to *Swift* SGRBs, the k-correction, the maximum distance observed by a certain event, the jet opening angle and the provability of the event being SGRB. They obtained the event rate of $8^{+5}_{-3} \times 10^{-9}$–$1.1^{+0.7}_{-0.47} \times 10^{-6}$ events Mpc^{-3}yr^{-1} for the case of isotropic emission and beamed emission, respectively. In our analysis the minimum event rate is $\sim 4\times10^{-8}$ events Mpc^{-3}yr^{-1} after the geometrical correction of beaming angle, while the realistic one is $\sim 1.6 \times 10^{-7}$ events Mpc^{-3}yr^{-1}. Although both analysis used completely different methods, they are consistent with each other. For NS-NS binary, the detection range of adv-LIGO will be ~ 100 Mpc in 2016-2017 (Barsotti 2013) so that there is a good chance of the first gravitational wave detection around 2017.

ACKNOWLEDGMENTS

This work is supported in part by the Grant-in-Aid from the Ministry of Education, Culture, Sports, Science and Technology (MEXT) of Japan, No. 23540305, No. 24103006 (TN), No. 20674002 (DY), No. 23740179, No. 24111710, and No. 24340048 (KT).

REFERENCES

Amati, L., Frontera, F., Tavani, M, et al. 2002, A&A, 390, 81
Amati, L., 2006, MNRAS, 372, 233
Band, D.L., Matteson, J., Ford, L., et al. 1993, ApJ, 413, 281
Barsotti, L. 2013 Talk at GWPAW, Pune, India 17-20, Dec. 2013
Berger, E. 2013 arXiv:1311.2603
Coward, D.M. , Howell, E.J., Piran, T. et al. 2012, MNRAS, 425, 2668
Dainotti, M. G., Petrosian, V., Singal, J., et al., 2008,
Efron, B. & Petrosian, V., 1992, ApJ, 399, 345
Fong, W., Berger, Margutti, R. et al. 2012, ApJ, 756, 189
Fong, W., Berger, E.,Chornock, R. et al. 2013a, ApJ, 769, 56
Fong, W., Berger, E.,Metzger, B.D. et al. 2013b, arXiv:1309.7479
Ghirlanda, G., Ghisellini, G., Lazzati, D., 2004, ApJ, 616, 331
Ghirlanda, G., Ghisellini, G., Firmani, C., 2005a, MNRAS, 361, L10; astro-ph/0502186
Ghirlanda, G. et al., 2005b, MNRAS, 360, L45
Ghirlanda, G., Nava, L., Ghisellini, G., et al. 2009, A&A, 496, 585-595
Harrison, F. A., Bloom, J. S., Frail, D. A. et al. 1999, ApJ, 523, 121
Kalogera, V., Kim, C., Lorimer, D. R. et al. 2004, ApJ, 601, L179
Kalogera, V., Kim, C., Lorimer, D. R. et al. 2004, ApJ, 614, L137
Kaneko, Y., Preece, R. D., Briggs, M. S., et al. 2006, ApJS, 166, 298
Krimm, H. A., et al. 2009, ApJ, 704, 1405
Lloyd-Ronning, N. M., Petrosian, V. & Mallozzi, R. S., 2001, ApJ, 534, 227
Lynden-Bell, D., 1971, MNRAS, 155, 95
Maloney, A. & Petrosian, V., 1999, ApJ, 518, 32
Nicuesa Guelbenzu, A., Klose, S., Rossi, A. et al. 2011, A&A, 531, L6
Petrosian, V., 1993, ApJ, 402, L33
Rhoads, J. E. 1999, ApJ, 525, 737
Seto, N., Kawamura, S., & Nakamura, T. 2001, Physical Review Letters, 87, 221103
Soderberg, A. M., Berger, E., Kasliwal, M. et al. 2006, ApJ, 650, 261
Tanvir, N. R., Fox, D. B., Levan, A. J. et al. 2009, Nature, 461, 1254
Tsutsui, R., Yonetoku, D., Nakamura, T. et al. 2013, MNRAS, 431, p.1398
Yonetoku, D., Murakami, T., Nakamura, T. et al., 2004, ApJ, 609, 935
Yonetoku, D., Murakami, T., Tsutsui, R. et al., 2010, PASJ, 62, 1495

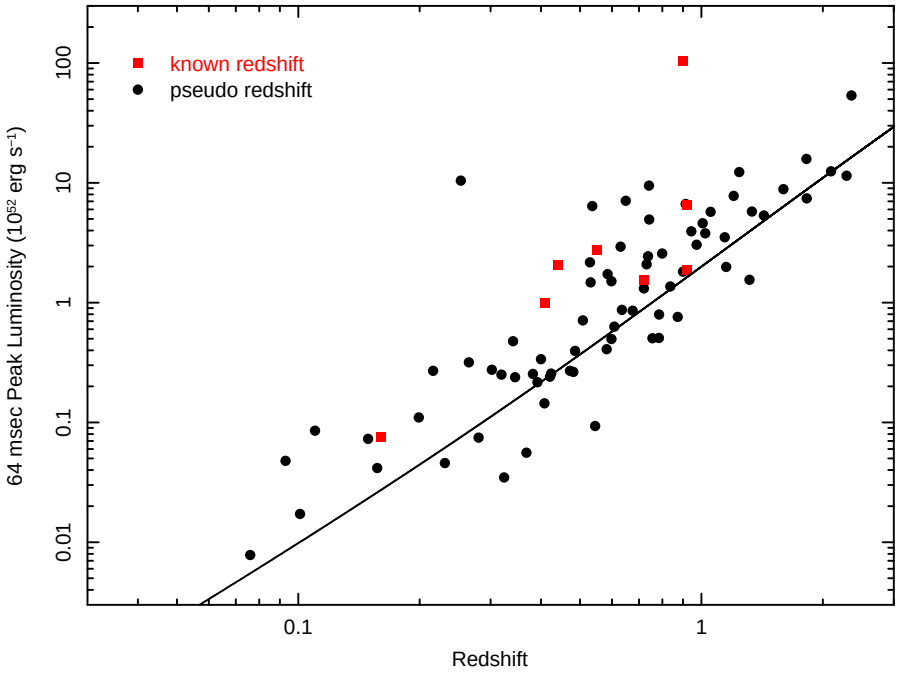

FIG. 1.— The redshift distribution of SGRBs estimated by the E_p–luminosity correlation by (Tsutsui et al. 2013). The solid squares are known redshift samples, and the solid circles are ones of pseudo redshift. The solid line is the flux limit of 4×10^{-6} erg cm^{-2}s^{-1}

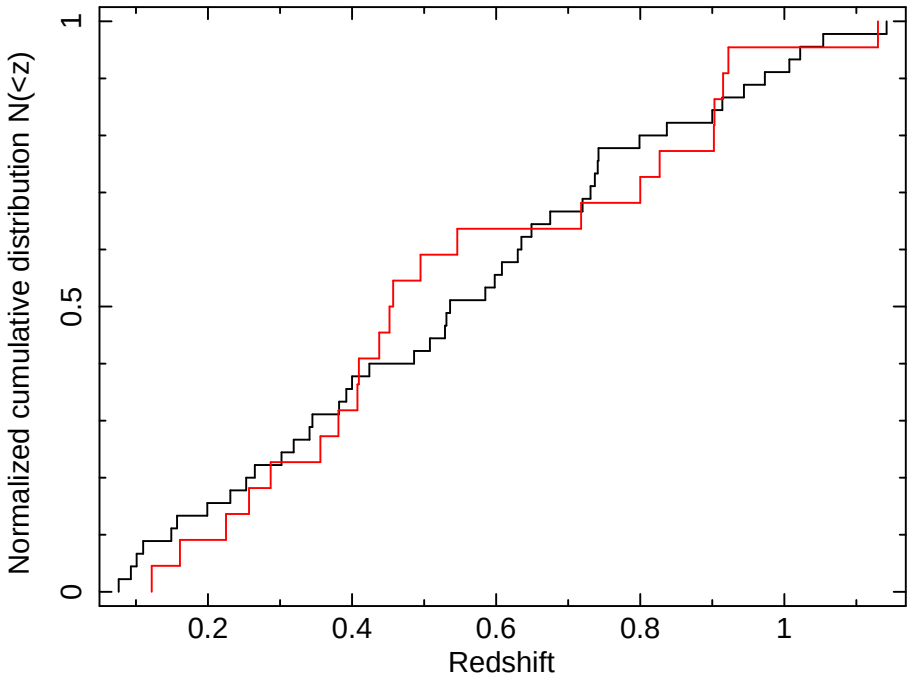

FIG. 2.— The cumulative redshift distribution of SGRBs up to $z = 1.14$. The black and the red solid lines are for 45 BATSE SGRBs in this paper and 22 known redshift samples observed by HETE-2 and *swift*/BAT, respectively. We can see the very good agreement of black and red lines up to $z \sim 0.4$. Kolmogorv-Smirnov test shows that the probability that the two curves for $z < 0.4$ arise from different distribution is 5.3 %, which is quite low for this number of samples. This strongly suggests that the E_p–L_p correlation for SGRB (Tsutsui et al. 2013) is a good distance indicator.

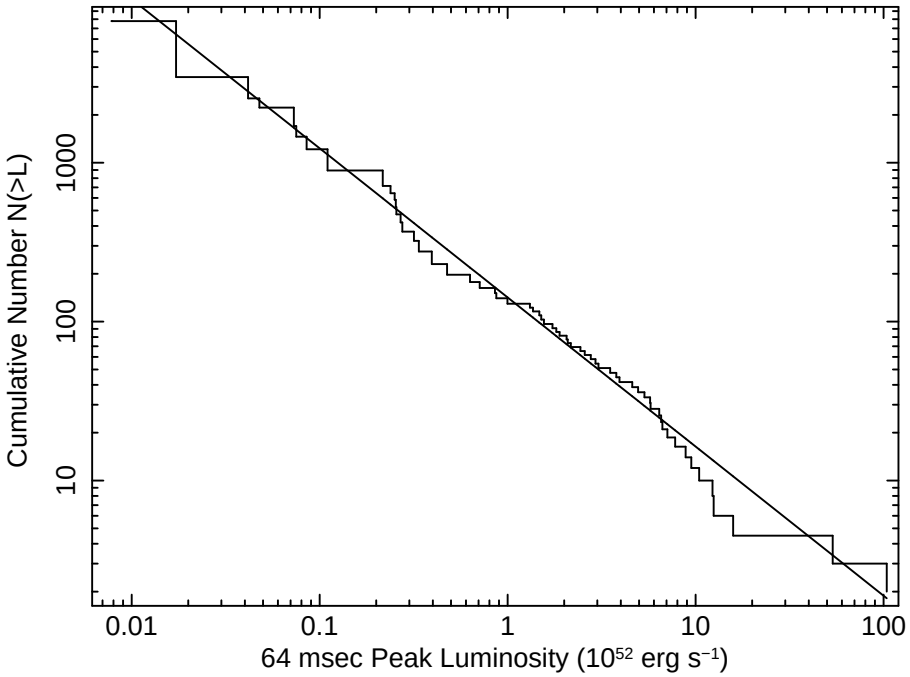

FIG. 3.— The luminosity function of SGRBs estimated from data distribution of figure 1. We can approximately describe it as a simple power-law function with the index of -1, and no obvious break has not been found.

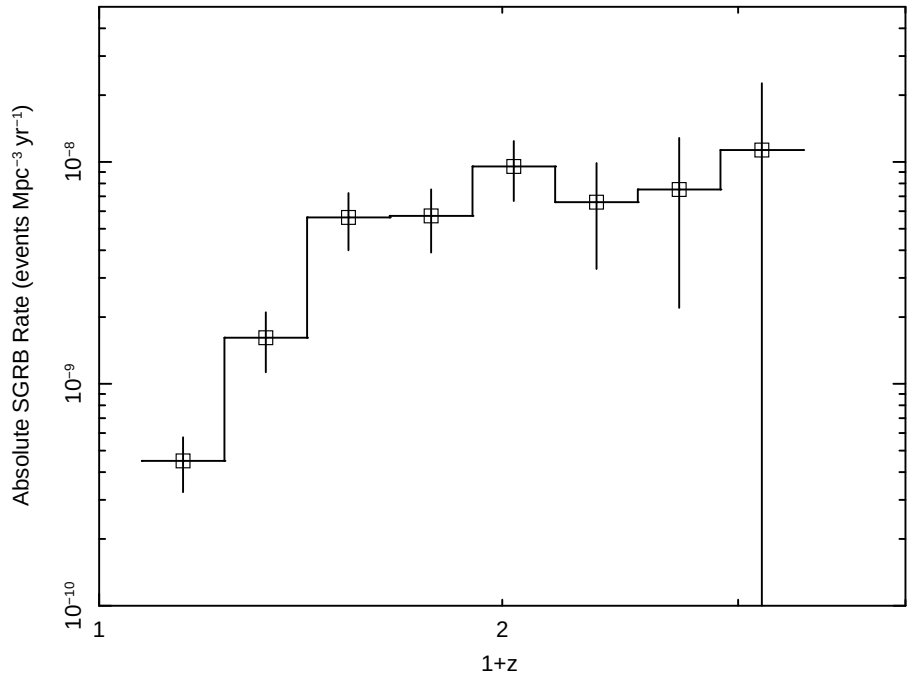

FIG. 4.— Absolute formation rate of SGRBs estimated from data distribution of figure 1. The local event rate at $z = 0$ is $\rho(0) = 2 \times 10^{-10}$ events $\mathrm{Mpc}^{-3}\mathrm{yr}^{-1}$.